BIOCHEMISTRY
including biophysical chemistry & molecular biology

Article

pubs.acs.org/biochemistry

Structure and Function of a Decarboxylating *Agrobacterium tumefaciens* Keto-deoxy-D-galactarate Dehydratase

Helena Taberman,[†] Martina Andberg,[‡] Tarja Parkkinen,[†] Janne Jänis,[†] Merja Penttilä,[‡] Nina Hakulinen,[†] Anu Koivula,[‡] and Juha Rouvinen*,[†]

[†]Department of Chemistry, University of Eastern Finland, FI-80101 Joensuu, Finland
[‡]VTT Technical Research Centre of Finland, FI-02044 VTT, Finland

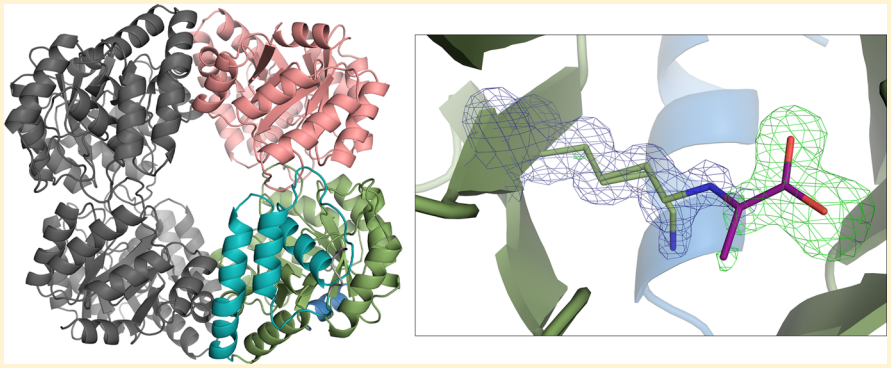

ABSTRACT: *Agrobacterium tumefaciens* (*At*) strain C58 contains an oxidative enzyme pathway that can function on both D-glucuronic and D-galacturonic acid. The corresponding gene coding for *At* keto-deoxy-D-galactarate (KDG) dehydratase is located in the same gene cluster as those coding for uronate dehydrogenase (*At* Udh) and galactarolactone cycloisomerase (*At* Gci) which we have previously characterized. Here, we present the kinetic characterization and crystal structure of *At* KDG dehydratase, which catalyzes the next step, the decarboxylating hydrolyase reaction of KDG to produce α-ketoglutaric semialdehyde (α-KGSA) and carbon dioxide. The crystal structures of *At* KDG dehydratase and its complexes with pyruvate and 2-oxoadipic acid, two substrate analogues, were determined to 1.7 Å, 1.5 Å, and 2.1 Å resolution, respectively. Furthermore, mass spectrometry was used to confirm reaction end-products. The results lead us to propose a structure-based mechanism for *At* KDG dehydratase, suggesting that while the enzyme belongs to the Class I aldolase protein family, it does not follow a typical retro-aldol condensation mechanism.

Producing fuels and chemicals from renewable materials would allow oil independency and reduction of greenhouse gas emissions. Plant biomass provides a rich source of sugars that can be converted through microbial pathways to useful platform chemicals. The main focus has so far been in biotechnical processes, which utilize sucrose, starch, or cellulose-derived D-glucose. However, the less explored sugars from hemicellulose and pectin should also be considered. Pectin is a heteropolysaccharide, rich in the cell walls of, for example, citrus species and sugar beet, and composed of mainly D-galacturonate and small amounts of D-xylose, D-galactose, L-arabinose, and L-rhamnose.[1] D-Galacturonate is a carbon and energy source for many bacterial and fungal species. Various catabolic D-galacturonate pathways have been described in microbes, and two of them are found in bacteria: the isomerase and the oxidative pathway.[2] The oxidative pathway has been described originally for *Agrobacterium tumefaciens* (*At*) and *Pseudomonas syringae*;[3,4] however, no genes were identified at the time.

We and others have recently shown that the enzymatic oxidation of D-galacturonate in *A. tumefaciens* can be carried out using novel enzyme reactions in the following manner (Figure 1): First NAD^+-dependent uronate dehydrogenase (*At* Udh, EC 1.1.1.203) oxidizes the pyranose form of D-galacturonate to D-galactaro-1,5-lactone,[5,6] which is isomerized either non-enzymatically or by a D-galactarolactone isomerase (*At* GLI) to D-galactaro-1,4-lactone.[6,7] D-Galactaro-1,4-lactone is then converted by a novel ring opening reaction into a linear keto-deoxy-D-galactarate (KDG; systematic name 3-deoxy-L-*threo*-2-hexulosarate) catalyzed by galactarolactone cycloiosomerase (*At* Gci, EC 5.5.1.-).[8] The *At* KDG dehydratase (EC 4.2.1.-) characterized here is supposed to produce from the linear C6 compound α-ketoglutaric semialdehyde a C5 compound (Figure 1).[9] The last step in the oxidative pathway should involve oxidation of α-ketoglutaric semialdehyde to α-ketoglutarate by an α-ketoglutaric semialdehyde (α-KGSA) dehydrogenase (EC 1.2.1.26).[10,11] The α-ketoglutarate then enters the tricarboxylic acid cycle.[10]

Received: October 14, 2014
Revised: November 26, 2014
Published: December 2, 2014

dx.doi.org/10.1021/bi501290k | *Biochemistry* 2014, 53, 8052−8060

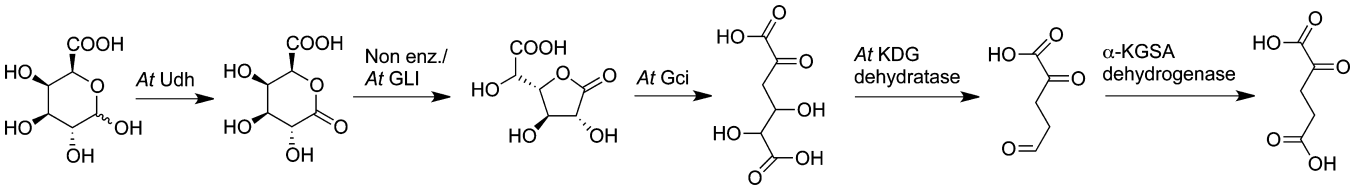

Figure 1. Oxidative pathway of D-galacturonate in *Agrobacterium tumefaciens*.

At KDG dehydratase belongs to the Class I aldolase protein family. This family has been reported to contain a number of enzymes, for example, *N*-acetylneuraminate lyase, that catalyzes condensation of pyruvate with *N*-acetyl-D-mannosamine, dihydrodipicolinate synthase (DHDPS) that catalyzes the condensation of L-aspartate-4-semialdehyde and pyruvate, *trans-o*-hydroxybenzylidenepyruvate hydratase-aldolase that splits 4-(2-hydroxyphenyl)-2-oxobut-3-enoate to salicylaldehyde and pyruvate, and D-4-deoxy-5-oxoglucarate dehydratase (DOGDH) that catalyzes an identical reaction as *At* KDG dehydratase.[12] So far there are no crystal structures and only a few kinetic characterization work of the DOGDH-type of enzymes published.[11,13,14]

Here, we present, to our knowledge, the first crystal structure for a DOGDH-type enzyme, namely, that for *At* KDG dehydratase. The closest related structure in the Protein Data Bank (PDB), DHDPS of *Agrobacterium tumefaciens* (PDB ID: 4I7U, no publication yet), has only 30% sequence identity with *At* KDG dehydratase. We have determined the crystal structures of *At* KDG dehydratase without ligand and in complex with pyruvate and 2-oxoadipic acid, two substrate analogues, to 1.7 Å, 1.5 Å, and 2.1 Å resolutions, respectively. The kinetic properties have also been characterized and mass spectrometry was used to confirm reaction end-products. Furthermore, mutagenesis of an active site residue, Ser211, was carried out. The results lead us to propose a structure-based mechanism for the enzymatic decarboxylation and dehydration of KDG by *At* KDG dehydratase.

EXPERIMENTAL PROCEDURES

Heterologous Protein Production and Mutagenesis. Production and purification of *At* KDG dehydratase were performed as described previously.[9] Briefly, the *At kdg* gene with a C-terminal *Strep*-tag II was expressed in *Escherichia coli* BL21(DE3) cells, and the enzyme was purified from the cell extract in a single step using a *Strep* Tactin Superflow column.

Site-directed mutation of Ser211 to alanine was introduced into the *Strep* II-tagged *At kdg* gene in the pBAT4 vector.[9] The mutagenesis was performed using the Quick Change Site-Directed mutagenesis kit (Stratagene, La Jolla, CA) according to the manufacturer's instructions. The nucleotide sequence of the mutated gene was confirmed by DNA sequencing. The mutated plasmid DNA was transformed into BL21(DE3) *E. coli* cells, and the *Strep*-tagged Ser211Ala mutant was expressed in *E. coli* and purified using essentially the same protocol as for the wild-type enzyme.[9] The activity of the purified Ser211Ala mutant was assayed at pH 7.5, at 22 °C in a coupled assay using *Acinetobacter baylyi* ADP1 α-ketoglutaric semialdehyde dehydrogenase, as described for the wild-type enzyme.[9,11]

pH Optimum. For determination of the pH optimum, KDG substrate was first produced from galactaric acid in 50 mM Tris-HCl pH 8, in a separate reaction using *Salmonella typhimurium* talarate/galactarate dehydratase.[9,15] The activity of the *At* KDG dehydratase was assayed at 22 °C in a coupled assay using *Acinetobacter baylyi* ADP1 α-ketoglutaric semialdehyde dehydrogenase, basically as described earlier.[9,11] KDG was incubated with 1 μg of *At* KDG dehydratase and 5 μg of *A. baylyi* α-ketoglutaric semialdehyde dehydrogenase in McIlvaine buffer (pH 4−7.5), Tris-HCl buffer (pH 6.5−9.5), and sodium phosphate buffer (pH 7−9) in a total volume of 100 μL. The activity was measured by following the formation of NADPH at 340 nm.

Kinetics of At KDG Dehydratase. Kinetic constants (K_m and k_{cat} values) for *At* KDG dehydratase were determined on KDG using a coupled enzyme assay (described above), and 100 mM NaCl and 4 mM NADP in 50 mM sodium phosphate buffer pH 7.5 at 22 °C. Fourteen different substrate concentrations (0.006 to 5 mM) were used and the kinetic measurements were performed in triplicate in microtiter plates in a total volume of 100 μL. The reactions were started by addition of the substrate, and the reduction of the cofactor was followed at 340 nm over 5 min using a Varioskan kinetic plate reader (Thermo Electron Corporation, USA). The kinetic parameters were obtained by curve fitting analysis using Prism software 6.02 (GraphPad, La Jolla, CA, USA).

Protein Oligomerization by Dynamic Light Scattering. Analysis of the oligomeric state of *At* KDG dehydratase was done by dynamic light scattering at 22 °C using DynaPro99 dynamic light scattering system (Wyatt Technology Corp., Santa Barbara, CA, USA) with a temperature-controlled microsampler. The filtered *At* KDG dehydratase (2 mg/mL) was scanned 20 times per measurement, and this was performed in triplicate.

Crystallization. The crystallization procedure of *At* KDG dehydratase was performed as described previously.[9] Briefly, all crystals were grown by the hanging drop vapor diffusion method at 20 °C by mixing 2 μL of 5 mg/mL enzyme in 50 mM Tris-HCl buffer (pH 7.5) with an equal volume of reservoir solution and equilibrated against 0.5 mL of reservoir solution. The crystallization conditions contained 0.1 M BICINE pH 8.5 buffer, 0.2 M sodium formate, and 15% (*w*/*v*) polyethylene glycol monomethyl ether 5000. Under these conditions, three-dimensional crystals grew in few days to dimensions ~0.4 × 0.2 × 0.2 mm^3. These crystals were used for the crystal structure determination of *At* KDG dehydratase, and also for the soaking experiments with pyruvate and 2-oxoadipic acid complex structures. The complex structures were prepared by soaking the crystals in cryoprotectant solution (reservoir solution containing 15% (*v*/*v*) glycerol) containing 10 mM pyruvate or 50 mM 2-oxoadipic acid in addition. After a 1 to 2 min soak in the cryoprotectant solution, the crystals were flash-cooled by plunging into liquid nitrogen.

X-ray Data Collection and Processing. After the crystals were cooled in liquid nitrogen the X-ray diffraction data were collected at 100 K with synchrotron radiation sources; for *At* KDG dehydratase structure without ligand at European Synchrotron Radiation Facility (ESRF) at beamline ID29,[16] and for the pyruvate and the 2-oxoadipic acid complex

dx.doi.org/10.1021/bi501290k | *Biochemistry* 2014, 53, 8052−8060

Table 1. Data Collection and Refinement Statistics[a]

	without ligand	pyruvate	2-oxoadipic acid
Beamline	ID29 (ESRF)	I03 (Diamond)	I04−1 (Diamond)
PDB code	4UR5	4UR7	4UR8
Space Group	C2	C2	C2
Unit cell [*a*,*b*,*c* (Å), β (deg)]	168.9, 118.4, 74.3 112.3	169.8, 120.1, 74.1 112.0	169.5, 119.0, 74.3 112.2
Resolution (Å)	47.71−1.65 (1.75−1.65)	48.09−1.50 (1.54−1.50)	47.90−2.10 (2.15−2.10)
No. of observed reflections	550817 (86097)	604602 (41544)	272290 (19355)
No. of unique reflections	159523 (25113)	214991 (15841)	76785 (5470)
Redundancy	3.5 (3.4)	2.8 (2.6)	3.5 (3.5)
Completeness (%)	98.1 (95.6)	97.7 (97.4)	96.0 (92.8)
R_{merge} (%)	7.2 (57.8)	3.8 (50.9)	13.6 (71.0)
$CC_{1/2}$	99.6 (80.4)	99.9 (79.4)	98.8 (71.3)
$I/\sigma I$	10.0 (2.0)	15.6 (2.3)	8.4 (2.0)
R_{work} (%)/R_{free} (%)	17.4/20.4	16.3/18.2	22.1/27.2
No. of atoms	10508	10963	9603
Protein	9241	9312	9157
Water	1216	1559	400
Pyruvate		20	
2-Oxoadipic acid			40
Glycerol	42	60	
Formate	9	12	6
Wilson *B*-factor	22.4	18.3	28.3
Average *B*-factor (Å^2)	26.9	23.7	32.5
Protein	25.8	21.9	32.5
Pyruvate		21.0	
2-Oxoadipic acid			34.0
rmsd bond lengths (Å)	0.007	0.006	0.009
rmsd bond angles (deg)	1.1	1.1	1.2
Ramachadran plot (%)			
Most favored	92.6	92.5	91.7
Additionally allowed	6.3	6.3	7.3

[a]Values in parentheses are for highest resolution shell.

structures at Diamond Light Source at beamlines I03 and I04−1, respectively. All the diffraction data sets were processed using XDS, and the data sets for the complex structures were also scaled with XSCALE.[17]

Structure Determination and Refinement. The phase problem of the *At* KDG dehydratase was solved with molecular replacement using MOLREP[18] from the CCP4 program suite.[19] The structure of *Bacillus clausii* DHDPS (PDB ID: 3E96, no publication yet) that has only 28% sequence identity to *At* KDG dehydratase was used as a search model. This was followed by a rigid body refinement with REFMAC5[20] also from the CCP4 program suite. The initial structure was then better fitted into the electron density map with AutoBuild.[21] The model building was completed manually with COOT,[22] and the refinement was performed with PHENIX.[23] The complex structures of *At* KDG dehydratase with pyruvate and 2-oxoadipic acid were also solved by molecular replacement with Phaser[23] using the structure of *At* KDG dehydratase without ligand as a template. The model building and refinement was carried out and the ligand molecules added into the excess electron densities. The validation of all the models was performed with MolProbity.[24] The data collection and refinement statistics are summarized in Table 1. The atomic coordinates and the experimental structure factor amplitudes have been deposited in the PDB in Europe.[25]

Mass Spectrometry. The reaction end-product measurements were performed on quadrupole ion trap (QIT) instrument (Esquire 3000 Plus, Bruker Daltonics, Bremen, Germany) operated in negative-ion mode. The instrument has been described in detail previously.[26] A 1 mL mixture of 1 mM substrate in water and 2 μL of enzyme (5 mg/mL) was prepared, and left to stand at room temperature for 30 min. The reactions were done using both the wild-type *At* KDG dehydratase and the Ser211Ala mutant. The reactions were stopped by diluting the mixtures with acetonitrile (1:20, *v*/*v*) and directly analyzed using electrospray ionization (ESI) at a flow rate of 160 μL/h. All observed ions were subjected to collision-induced dissociation (CID) tandem mass spectrometry (MS/MS) experiments for further identification. The instrument was controlled and the data were processed using Bruker Daltonics Compass 1.1 for Esquire/HCT software. The spectra were further analyzed with Bruker DataAnalysis 4.1 software.

RESULTS

Biochemical Characterization of At KDG Dehydratase. *At* KDG dehydratase was expressed in *E. coli* and purified using the *Strep*-tag II one-step purification system. The yield from one liter of cell culture was approximately three milligrams of purified protein. The pH optimum of the purified *At* KDG dehydratase was determined using enzymatically produced KDG as a substrate. *At* KDG dehydratase was shown to have optimal activity in the range of pH 7.5 to 8 (Figure 2A).

The stability of the purified *At* KDG dehydratase was analyzed as a function of temperature. The enzyme was found to retain more than 60% of its activity after 22 h at 40 °C. At 50

dx.doi.org/10.1021/bi501290k | *Biochemistry* 2014, 53, 8052−8060

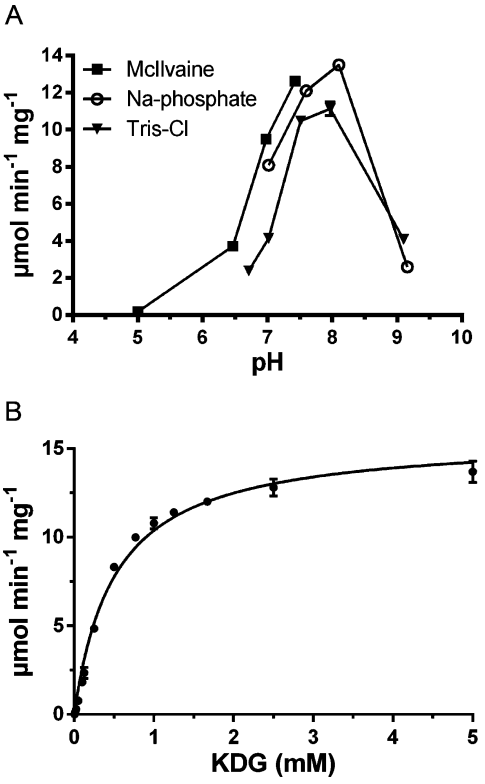

Figure 2. (A) pH optimum of *At* KDG dehydratase measured at 22 °C using KDG as a substrate. The enzyme was incubated in McIlvaine's buffer (filled squares), sodium phosphate buffer (open circles), or Tris-Cl buffer (filled triangles). (B) Kinetic properties of the purified *At* KDG dehydratase. Kinetic data were obtained from incubations of 1 μg *At* KDG dehydratase and 5 μg *A. baylyi* α-ketoglutaric semialdehyde dehydrogenase with KDG (0.006−5 mM, 100 mM NaCl, 4 mM NADP) in sodium phosphate buffer pH 7.5 at 22 °C. The apparent kinetic parameters were obtained by curve fitting analysis using GraphPad Prism software 6.02.

°C the activity was reduced to 20% after 22 h, whereas less than 1% activity was detected after 30 min at 70 °C (data not shown). The enzyme was expected to be stable at 22 °C, and therefore the kinetic analysis on KDG was carried out at this temperature. The determined K_m value of *At* KDG dehydratase was 0.50 ± 0.03 mM, k_{cat} was 530 ± 10 min^{-1}, and the specificity constant (k_{cat}/K_m) was 1.02 × 10^6 M^{-1} min^{-1} (Figure 2B).

Structure Determination. The crystals of *At* KDG dehydratase belonged to the monoclinic space group C2 with the following unit-cell parameters: a = 168.9, b = 118.4, c = 74.3 Å, β = 112.3°. The Matthews coefficient[27] was approximately 2.5 $Å^3$/Da, which corresponds to four monomers in the asymmetric unit with an estimated solvent content of 51%. The structure of *At* KDG dehydratase without ligand was processed to 1.7 Å resolution and the phases were obtained by molecular replacement. *At* KDG dehydratase monomer consisted of 303 residues (without the *Strep*-tag). The final solved structure was composed of 1219 amino acid residues, 1216 water molecules, 7 glycerol molecules, and 3 formate molecules. The structure was refined to R_{work} value of 17% and R_{free} value of 20%. The root-mean-square differences (rmsd) between the monomers were ∼0.3 Å. A part of the *Strep*-tag II (Trp-Ser-His-Pro-Gln-Phe-Glu-Lys), added at the C-terminus of *At* KDG dehydratase to aid the protein purification, was also visible in the electron density.

The structures of *At* KDG dehydratase in complex with pyruvate and 2-oxoadipic acid were determined by soaking the crystals with a cryoprotectant solution containing the ligand at issue. The complex structure with pyruvate was determined to 1.5 Å resolution, R_{work} value was 16%, and R_{free} value was 18%. The resolution of the complex structure with 2-oxoadipic acid was 2.1 Å with R_{work} value of 22% and R_{free} value of 27%. The rmsd values between the molecules and the models were ∼0.4 Å.

Overall Structure. *At* KDG dehydratase monomer consists of twelve α-helices and eight β-strands (Figure 3A). The structure contains an α/β-barrel domain with eight parallel β-strands (β1−β8) surrounded by eight α-helices (α1−α8). At the N-terminus an α-helix (αN) packs against the N-terminal side of the β-barrel, and at the C-terminus there is an extension of three α-helices (αC1−3) that are also involved in the formation of the quaternary structure. The substrate-binding site is located at the C-terminal side of the β-barrel.

The analysis of the oligomerization of *At* KDG dehydratase with the interactive tool PDBePISA[28] suggested that the enzyme formed a tetramer with a total interface area of ∼4860 $Å^2$. Two monomers formed a tightly packed dimer with an interface area of approximately 1580 $Å^2$. The interface area included the long loop between the β4 and α4, which penetrated to the second monomer. Two dimers were then more loosely packed together, which resulted in two new monomer−monomer interfaces of ∼850 $Å^2$. These interfaces were relatively flat and consisted mainly of three α-helices (α6, α7, and αC1). The complete *At* KDG dehydratase tetramer had a 222 symmetry (Figure 3B). As determined by dynamic light scattering, *At* KDG dehydratase was also found to be a tetramer in solution (data not shown).

Ligand Binding. Co-crystallization or soaking of *At* KDG dehydratase crystals with the substrate or the product did not result in additional electron density in the active site. However, cryoprotection with a pyruvate containing solution resulted in covalent attachment of the ligand with the conserved Lys166, which was located at the C-terminus of the β5. This helped to identify the location of the active site of the enzyme. The imine form was chosen to be used in the refinement of both of the ligands, pyruvate and 2-oxoadipic acid, according to the electron densities and the binding geometries (hydrogen bonds). The electron density maps ($2F_o-F_c$ map around Lys166 and F_o-F_c omit map around the ligand) of the formed Schiff-bases of Lys166 covalently bound to the two ligands are shown in Figure 3C and D.

In the noncomplexed form the ε-amino group of the lysine side-chain formed a hydrogen bond to Tyr140 (Figure 4A). This hydrogen bond did not exist in either one of the complex structures, but instead the Lys166 formed the covalent bond to the ligand. In the case of the ligand being pyruvate the Shiff-base formation and the occupancy of pyruvate were, however, only partial and the Lys166 had also a nonbonded conformation in which the ε-amino group of the lysine side-chain formed a hydrogen bond to Ser211 (Figure 4B). The carboxylate group of the pyruvate formed hydrogen bonds with the main chain nitrogens of Gly53 and Thr54, and with the side-chain hydroxyl group of Thr54 (see Figure 4B). This Gly-Thr motif was located in the loop between the β2 and α2.

2-Oxoadipic acid was selected as a ligand due to its structural similarity with the substrate, since it is only lacking the O4 and O5 hydroxyl groups as compared to KDG. The 2-oxoadipic acid complex structure showed a similar covalent bond

dx.doi.org/10.1021/bi501290k | *Biochemistry* 2014, 53, 8052−8060

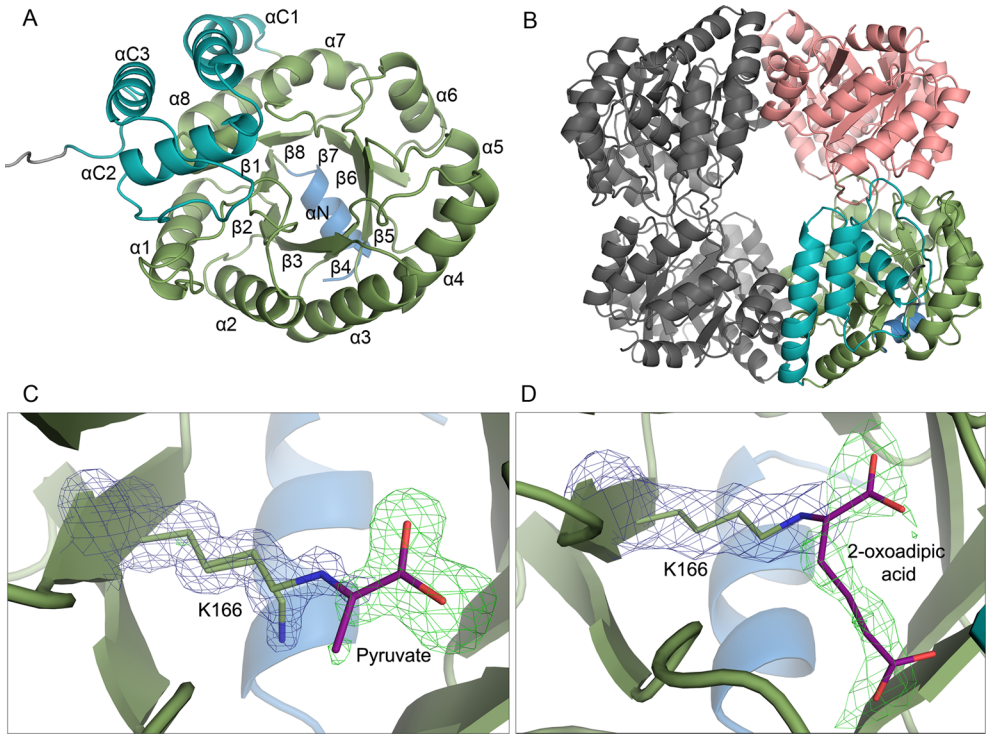

Figure 3. (A) Overall structure of the *At* KDG dehydratase monomer as a ribbon model. α/β-barrel in green, N-terminal helix in blue, C-terminal helices in cyan, and *Strep*-tag in gray. (B) Tetrameric structure of *At* KDG dehydratase. One of the monomers is colored as in (A). This has an extensive interface with a second monomer that is colored in light red. The dimer formed then packs together more loosely with the second half of the tetramer (in gray) forming a smaller interface. (C) Electron density map around the Schiff-base of Lys166 covalently bound to pyruvate. (D) Electron density map around the Schiff-base of Lys166 covalently bound to 2-oxoadipic acid. The $2F_o - F_c$ (blue) electron density maps around the Lys166 are contoured at 1σ, and the $F_o - F_c$ omit maps (green) around the ligands are contoured at 3σ.

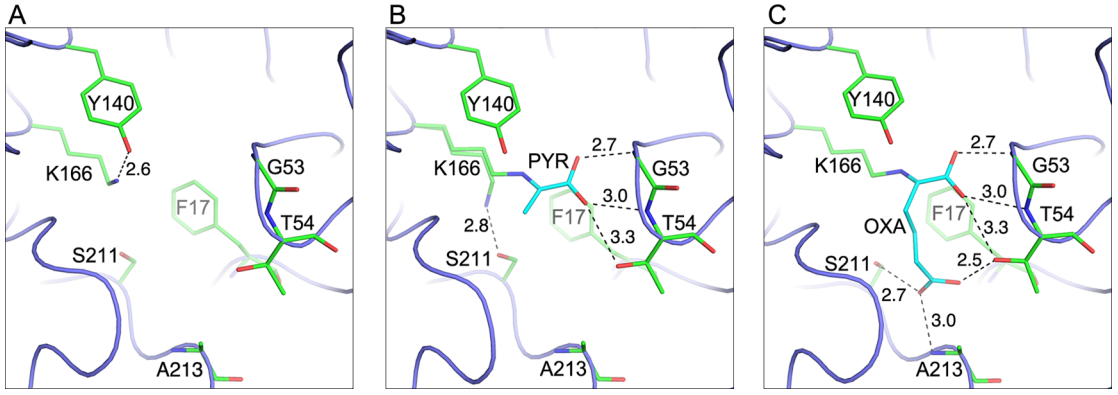

Figure 4. Comparison of the active sites of *At* KDG dehydratase in the three determined crystal structures. The residues are labeled and the hydrogen bonds are showed as dashed lines with the bond lengths (Å): (A) without ligand; (B) pyruvate (PYR) complex; (C) 2-oxoadipic acid (OXA) complex.

formation to Lys166 and interactions with Gly-Thr motif as did the pyruvate complex structure. According to the electron density map, the aliphatic chain of 2-oxoadipic acid has different conformations. Nevertheless, the most extensive electron density was found in the monomer C in which the aliphatic chain was bound in to the small cleft formed by the loops between β7 and α7, and β8 and α8 (Figure 4C). Carboxylate oxygen of the ligand made hydrogen bonds with the main chain amino groups of Thr54 and Ala213.

Active Site Mutation Ser211Ala. Ser211 is conserved in DOGDH-type enzymes, but not in the other Class I aldolase protein family enzymes.[12] It it also located in the vicinity of Lys166, the putative catalytic amino acid. The role of Ser211 was studied by mutating it to alanine. The specific activity of the purified Ser211Ala mutant on KDG was found to be approximately 30 times lower than the activity of the wild-type enzyme.

Reaction Product Analysis. Negative ion ESI-QIT mass spectrometry was used to analyze the reaction end-product(s) of the decarboxylation and dehydration reactions (Figure 5). The mass spectrum of the substrate, KDG (192 Da), showed a single intense peak at m/z 191, corresponding to the ion $[M - H]^-$. The substrate was measured again after a 30 min reaction with both the wild-type *At* KDG dehydratase and the Ser211Ala mutant. In both cases a peak at m/z 129 appeared in the spectra, which corresponded to the expected reaction

dx.doi.org/10.1021/bi501290k | *Biochemistry* 2014, 53, 8052−8060

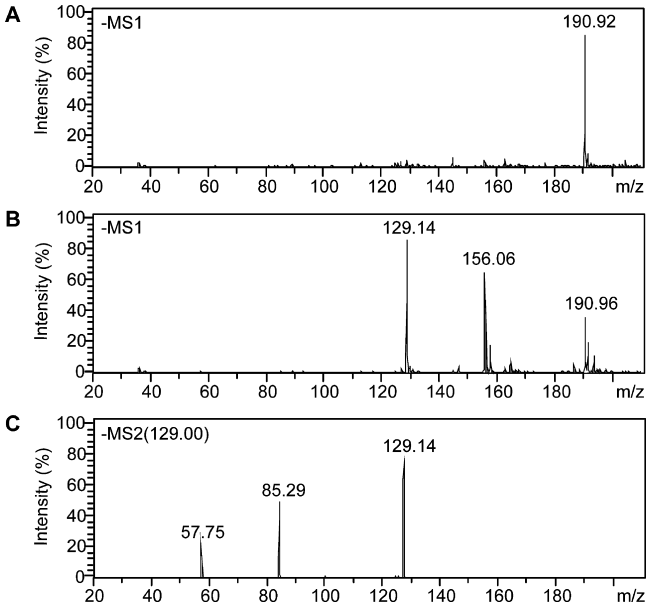

Figure 5. (A) ESI-MS spectrum of KDG. (B) ESI-MS spectrum of KDG after 30 min reaction with *At* KDG dehydratase. (C) ESI-MS/MS spectrum of the *At* KDG dehydratase reaction product (m/z 129). In B the ion at m/z 156/158 corresponds to the deprotonated Tris-HCl. In C the product ions at m/z 85 and 57 correspond to the neutral losses of carbon dioxide (44 Da) and carbon monoxide (28 Da).

product, α-ketoglutaric semialdehyde (130 Da), $[M - H]^-$ ion (m/z 129). The product ion structure was further verified by CID-MS/MS experiments (Figure 5). As a result we found ions at m/z 85 and 57, which corresponded to the neutral loss of carbon dioxide (44 Da) followed by the neutral loss of carbon monoxide (28 Da). The additional peak observed at m/z 156/158 corresponded to the deprotonated buffer salt, Tris-HCl (present in the enzyme solution). This is consistent with the enzymatic formation of α-ketoglutaric semialdehyde, and no other reaction products were observed. The only marked difference between the reaction spectra of the wild-type *At* KDG dehydratase and the Ser211Ala mutant was that the intensity of the product ion (m/z 129) was not as high with the Ser211Ala mutant as it was with the wild-type enzyme (data not shown). This supports the loss of activity with the mutation, shown already with the biochemical activity measurements.

DISCUSSION

We have shown recently that *Agrobacterium tumefaciens* strain C58 contains *At* Udh that oxidizes D-galacturonic acid to D-galactaro-1,5-lactone,[5,6] which is converted in solution to a more stable D-galactaro-1,4-lactone (Figure 1). In addition, a novel enolate family enzyme, *At* Gci, was found to convert the cyclic D-galactaro-1,4-lactone (but not the linear diacid form) to the L-*threo* form of KDG[8] (Figure 1). Besides D-galacturonic acid, *At* Udh was shown to be able to oxidize also D-glucuronic acid, and the formed D-glucuronolactone could be used by *At* Gci to produce the L-*threo* form of KDG. Here, we described the kinetic characterization, crystal structures, and reaction mechanism of *At* KDG dehydratase, which is the next enzyme in the oxidative pathway, also located in the same gene cluster as the two previously mentioned enzyme genes. Our results verify that *At* KDG dehydratase produces α-ketoglutaric semialdehyde, a C5 compound, from KDG. Furthermore, the crystal structures allow us to propose a reaction mechanism for the enzyme.

Reaction Mechanism. *At* KDG dehydratase catalyzes the net reaction, where the linear KDG is converted to α-ketoglutaric semialdehyde. In addition to the substrate, KDG, the reaction consumes one proton in oxidizing the substrate to α-ketoglutaric semialdehyde, carbon dioxide and water (Figure 6).

The members of this protein family catalyze reactions by forming an intermediate Schiff-base with their substrate and share a similar $(\alpha/\beta)_8$ barrel fold.[29,30] The characteristic feature for enzymes in the Class I aldolase protein family is the catalytic dyad consisting of nucleophilic lysine and a general acid/base residue, typically tyrosine.[29] In *At* KDG dehydratase these residues would be Lys166 from the β6 and Tyr140 from the β5. The reaction would start when the neutral side-chain of Lys166 makes a nucleophilic attack to the carbonyl C2 of the substrate (Figure 7) leading to the formation of imine. Deprotonation of β-carbon (C3) by a general base would then result in the enamine form of the substrate. We presume that the base catalyst in *At* KDG dehydratase is indeed Tyr140, because the phenolic oxygen of Tyr140 is near β-carbon of 2-oxoadipic acid (distance 3.6 Å) (Figure 8A).

Lawrence et al. have presented an overview on the reaction mechanism and suggested that dehydration and decarboxylation of enamine can occur simultaneously by protonation of the 4-hydroxyl.[12] Jeffcoat et al. presented that the elimination of 4-hydroxyl is favored by an intermediate in which a positive charge is located in the imine nitrogen.[14] We presume as Jeffcoat et al. that the elimination is of E1-type, because the cleaved bonds in the molecule are different (C−O and C−C).

Docking the enamine form of the substrate within the active site (Figure 8A) shows that the O4 hydroxyl would be close to Ser211. However, this serine would probably not be a catalytic acid because the serine hydroxyl has a very high pK_a value. The more probable role for Ser211 is to mediate the extraction of an acidic proton, needed in the reaction, from the solvent. Our results on Ser211Ala mutant showed decreased activity (by 30-fold) on KDG, which would also support the notion that this residue has a role in the catalysis, but it is not absolutely essential. In addition to the O4 hydroxyl protonation, the elimination reaction is especially favored, because the product formed would have a second double bond between C4−C5 conjugated with the enamine double bond between C2−C3.

Finally the reaction may proceed back to the imine form, to carbinol amine form, and consequently breaking of the covalent

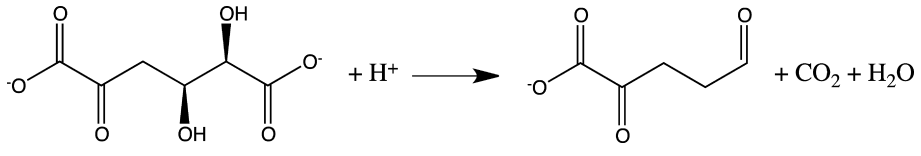

Figure 6. Net reaction of *At* KDG dehydratase.

dx.doi.org/10.1021/bi501290k | *Biochemistry* 2014, 53, 8052−8060

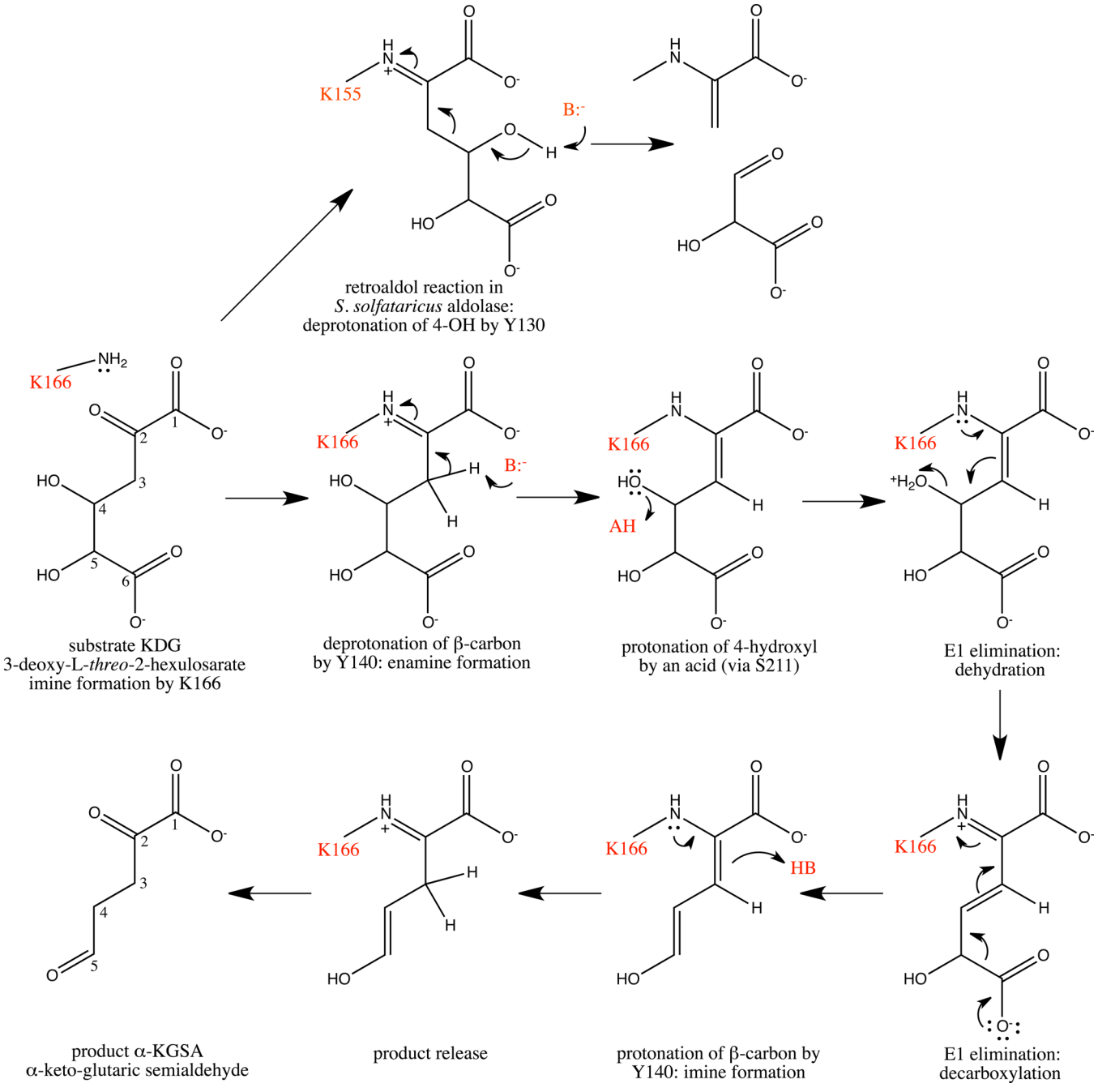

Figure 7. Proposed reaction mechanism for *At* KDG dehydratase.

bond between Lys166 and the product. Common keto−enol tautomerism interconverts the enol form to the product α-ketoglutaric semialdehyde (Figure 7).

Comparison with Aldolase. *At* KDG dehydratase shows sequence identity (23%) with 2-keto-3-deoxygluconate aldolase from *Sulfolobus solfataricus* (*Ss* KDGA, 31). Interestingly, this bacterial aldolase has a similar quaternary structure and it also uses the same substrate as *At* KDG dehydratase, but the *S. solfataricus* aldolase catalyzes retro-aldol reaction in which the C3−C4 bond of KDG is cleaved (Figure 7). The superimposition of the structures of *At* KDG dehydratase complexed with 2-oxoadipic acid, and *Ss* KDGA complexed with 3-deoxy-D-lyxohexonic acid (PDB ID: 1W3T) (Figure 8B) showed similar covalent binding of the conserved active site lysine residue to the ligand, but clearly different binding for the rest of the ligand. In *At* KDG dehydratase Phe17 interacts with the ligand, whereas in *Ss* KDGA Phe17 is replaced by Pro7, which inhibits ligand binding in this position. Ser211, which makes a hydrogen bond with the ligand in *At* KDG dehydratase, is also replaced with more bulky Val196 in *Ss* KDGA. In *Ss* KDGA the ligand interacts with Tyr132, which is replaced by the positively charged Arg142 in *At* KDG dehydratase. Finally, in *At* KDG dehydratase the Pro193 at the loop between β7 and α7 restricts the access to the active site. In *Ss* KDGA this loop is shorter, and extends the access to the active site.

The different catalytic reactions between *At* KDG dehydratase and *Ss* KDGA can be explained by differences in the orientations of covalently bound ligands toward acid/base catalyst tyrosine. In *Ss* KDGA O4 hydroxyl is close to the base catalyst, which leads to the proton abstraction and to retro-

dx.doi.org/10.1021/bi501290k | *Biochemistry* 2014, 53, 8052−8060

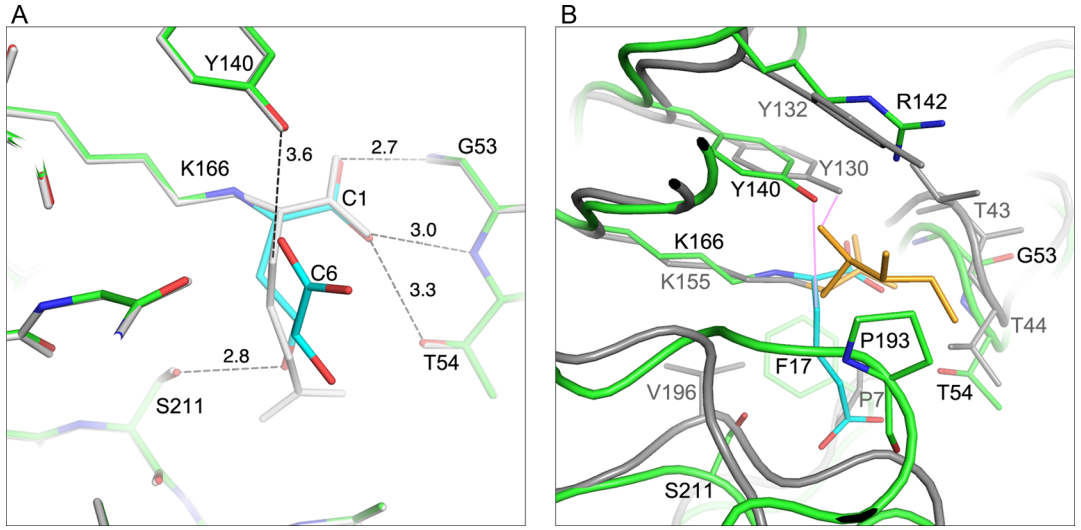

Figure 8. (A) Docked enamine intermediate (cyan) of the substrate in the active site of *At* KDG dehydratase (green). 2-Oxoadipic acid complex structure is in gray. The distance between the hydroxyl oxygen of Tyr140 and β-carbon of 2-oxoadipic acid is 3.6 Å. After deprotonation of the β-carbon an enamine is formed bringing O4 hydroxyl close to Ser211. (B) Superimposition of *At* KDG dehydratase (in green) complexed with 2-oxoadipic acid (in cyan) and KDGA (gray) complexed with 3-deoxy-D-lyxohexonic acid (orange) (PDB ID: 1W3T). The purple lines show the proposed proton abstraction by a general base, Tyr140.

aldol reaction. In *At* KDG dehydratase, the corresponding hydroxyl is tilted away and the C3 carbon is more close to the base catalyst, which leads to the proton abstraction from C3 carbon and enamine formation. The double bond at C2−C3 favors an elimination reaction through conjugation with the double bond at C4−C5 of the product intermediate.

In summary, three-dimensional structures of a Class I aldolase family enzyme *At* KDG dehydratase and its complexes with pyruvate and 2-oxoadipic acid, two substrate analogues along with the activity measurements, add to our understanding of the structure and function of *At* KDG dehydratase and its role in the enzymatic oxidative pathway of uronic acids. Our results on this novel type of decarboxylating hydrolyase enzyme should also promote further biotechnical applications and engineering efforts.

■ ASSOCIATED CONTENT

Accession Codes

The atomic coordinates and structure factors (codes: 4UR5, 4UR7, 4UR8) have been deposited in the Protein Data Bank in Europe (http://www.ebi.ac.uk/pdbe/). The oligomerization and the total interface area were determined with the 'Protein interfaces, surfaces and assemblies' service PISA at the European Bioinformatics Institute (http://www.ebi.ac.uk/pdbe/prot_int/pistart.html).

■ AUTHOR INFORMATION

Corresponding Author

*Tel.: 358-40-7055105; Fax: 358-13-2513390; E-mail: juha.rouvinen@uef.fi.

Funding

This work was supported by the National Doctoral Programme in Informational and Structural Biology, and the Academy of Finland through the Finnish Centre of Excellence in White Biotechnology-Green Chemistry (Decision 118573). The research leading to these results has received funding also from the European Community's Seventh Framework Programme (FP7/2007−2013) under BioStruct-X (grant agreement N°283570).

Notes

The authors declare no competing financial interest.

■ ACKNOWLEDGMENTS

We thank Outi Liehunen (VTT Technical research Centre of Finland), and Merja Niemi and Ritva Romppanen (University of Eastern Finland) for technical assistance. We acknowledge the European Synchrotron Radiation Facility and the staff of beamline ID29, and Diamond Light Source and the staffs of beamlines I03 and I04-1 for provision of synchrotron radiation facilities and for assistance in using the beamlines. Chiara Gasparetti is thanked for measuring the data for the complex structure of *At* KDG dehydratase and 2-oxoadipic acid. Robert M. Badeau, Ph.D., of Aura Professional English Consulting, Ltd. (www.auraenglish.com) performed the language content editing of this manuscript.

■ ABBREVIATIONS

At, *Agrobacterium tumefaciens*; Udh, uronate dehydrogenase; Gci, galactarolactone cycloisomerase; KDG, keto-deoxy-D-galactarate; QIT, quadrupole ion trap; ESI, electrospray ionization; CID, collision-induced dissociation; MS/MS, tandem mass spectrometry; DOGDH, D-4-deoxy-5-oxoglucarate; *Ss* KDGA, keto-3-deoxygluconate aldolase from *Sulfolobus solfataricus*; rmsd, root-mean-square deviation; GLI, D-galactarolactone isomerase; α-KGSA, α-ketoglutaric semialdehyde

■ REFERENCES

(1) Ochoa-Villarreal, M., Aispuro-Hernández, E., Vargas-Arispuro, I., and Martínez-Téllez, M. Á. (2012) Plant cell wall polymers: Function, structure and biological activity of their derivatives. *Polymerization*, 63−86 InTech, Rijeka, Croatia.

(2) Richard, P., and Hilditch, S. (2009) D-Galacturonic acid catabolism in micro-organisms and its biotechnological relevance. *Appl. Microbiol. Biotechnol. 82*, 597−604.

(3) Zajic, J. E. (1959) Hexuronic dehydrogenase of Agrobacterium tumefaciens. *J. Bacteriol. 78*, 734−735.

(4) Kilgore, W. W., and Starr, M. P. (1959) Uronate oxidation by phytopathogenic pseudomonads. *Nature 183*, 1412−1413.
(5) Boer, H., Maaheimo, H., Koivula, A., Penttilä, M., and Richard, P. (2010) Identification in Agrobacterium tumefaciens of the D-galacturonic acid dehydrogenase gene. *Appl. Microbiol. Biotechnol. 86*, 901−909.
(6) Parkkinen, T., Boer, H., Jänis, J., Andberg, M., Penttilä, M., Koivula, A., and Rouvinen, J. (2011) Crystal structure of uronate dehydrogenase from Agrobacterium tumefaciens. *J. Biol. Chem. 286*, 27294−27300.
(7) Bouvier, J. T., Groninger-Poe, F. P., Vetting, M., Almo, S. C., and Gerlt, J. A. (2014) Galactaro δ-lactone isomerase: Lactone isomerization by a member of the amidohydrolase superfamily. *Biochemistry 53*, 614−616.
(8) Andberg, M., Maaheimo, H., Boer, H., Penttilä, M., Koivula, A., and Richard, P. (2012) Characterization of a novel Agrobacterium tumefaciens Galactarolactone cycloisomerase enzyme for direct conversion of D-galactarolactone to 3-deoxy-2-keto-L-threo-hexarate. *J. Biol. Chem. 287*, 17662−17671.
(9) Taberman, H., Andberg, M., Parkkinen, T., Richard, P., Hakulinen, N., Koivula, A., and Rouvinen, J. (2014) Purification, crystallization and preliminary X-ray diffraction analysis of a novel keto-deoxy-D-galactarate (KDG) dehydratase from Agrobacterium tumefaciens. *Acta Crystallogr. F70*, 49−52.
(10) Watanabe, S., Yamada, M., Ohtsu, I., and Makino, K. (2007) Alpha-ketoglutaric semialdehyde dehydrogenase isozymes involved in metabolic pathways of D-glucarate, D-galactarate, and hydroxy-L-proline: molecular and metabolic convergent evolution. *J. Biol. Chem. 282*, 6685−6695.
(11) Aghaie, A., Lechaplais, C., Sirven, P., Tricot, S., Besnard-Gonnet, M., Muselet, D., de Berardinis, V., Kreimeyer, A., Gyapay, G., Salanoubat, M., and Perret, A. (2008) New insights into the alternative D-glucarate degradation pathway. *J. Biol. Chem. 283*, 15638−15646.
(12) Lawrence, M. C., Barbosa, J. A. R. G., Smith, B. J., Hall, N. E., Pilling, P. A., Ooi, H. C., and Marcuccio, S. M. (1997) Structure and mechanism of a sub-family of enzymes related to N-acetylneuraminate lyase. *J. Mol. Biol. 266*, 381−399.
(13) Groninger-Poe, F. P., Bouvier, J. T., Vetting, M. W., Kalyanaraman, C., Kumar, R., Almo, S. C., Jacobson, M. P., and Gerlt, J. A. (2014) Evolution of enzymatic activities in the enolase superfamily: galactarate dehydratase-III from Agrobacterium tumefaciens C58. *Biochemistry 53*, 4192−4203.
(14) Jeffcoat, R., Hassall, H., and Dagley, S. (1969) Purification and properties of D-4-deoxy-5-oxoglucarate hydro-lyase (decarboxylating). *Biochem. J. 115*, 977−983.
(15) Yew, W. S., Fedorov, A. A., Fedorov, E. V., Almo, S. C., and Gerlt, J. A. (2007) Evolution of enzymatic activities in the enolase superfamily: L-talarate/galactarate dehydratase from Salmonella typhimurium LT2. *Biochemistry 46*, 9564−9577.
(16) de Sanctis, D., Beteva, A., Caserotto, H., Dobias, F., Gabadinho, J., Giraud, T., Gobbo, A., Guijarro, M., Lentini, M., Lavault, B., Mairs, T., McSweeney, S., Petitdemange, S., Rey-Bakaikoa, V., Surr, J., Theveneau, P., Leonard, G. A., and Mueller-Dieckmann, C. (2012) ID29: a high-intensity highly automated ESRF beamline for macromolecular crystallography experiments exploiting anomalous scattering. *J. Synchrotron Rad. 19*, 455−461.
(17) Kabsch, W. (2010) XDS. *Acta Crystallogr. D66*, 125−132.
(18) Vagin, A., and Teplyakov, A. (1997) MOLREP: an automated program for molecular replacement. *J. Appl. Crystallogr. 30*, 1022−1025.
(19) Collaborative Computational Project, Number 4 (1994) The CCP4 suite: programs for protein crystallography. *Acta Crystallogr. D50*, 760−763.
(20) Murshudov, G. N., Skubák, P., Lebedev, A. A., Pannu, N. S., Steiner, R. A., Nicholls, N. A., Wimm, M. D., Long, F., and Vagin, A. A. (2011) REFMAC5 for the refinement of macromolecular crystal structures. *Acta Crystallogr. D67*, 355−367.
(21) Terwilliger, T. C., Grosse-Kunstleve, R. W., Afonine, P. V., Moriarty, N. W., Zwart, P. H., Hung, L.-W., Read, R. J., and Adams, P. D. (2008) Iterative model building, structure refinement and density modification with the PHENIX AutoBuild wizard. *Acta Crystallogr. D64*, 61−69.
(22) Emsley, P., Lohkamp, B., Scott, W. G., and Cowtan, K. (2010) Features and development of Coot. *Acta Crystallogr. D66*, 486−501.
(23) Adams, P. D., Afonine, P. V., Bunkóczi, G., Chen, V. B., Davis, I. W., Echols, N., Headd, J. J., Hung, L. W., Kapral, G. J., Grosse-Kunstleve, R. W., McCoy, A. J., Moriarty, N. W., Oeffner, R., Read, R. J., Richardson, D. C., Richardson, J. S., Terwilliger, T. C., and Zwart, P. H. (2010) PHENIX: a comprehensive Python-based system for macromolecular structure solution. *Acta Crystallogr. D66*, 213−221.
(24) Chen, V. B., Aredall, W. B., III, Headd, J. J., Keedy, D. A., Immormino, R. M., Kapral, G. J., Murray, L. W., Richardson, J. S., and Richardson, D. C. (2010) MolProbity: all-atom structure validation for macromolecular crystallography. *Acta Crystallogr. D66*, 12−21.
(25) Velankar, S., Alhroub, Y., Alili, A., Best, C., Boutselakis, H. C., Caboche, S., Conroy, M. J., Dana, J. M., van Ginkel, G., Golovin, A., Gore, S. P., Gutmanas, A., Haslam, P., Hirshberg, M., John, M., Lagerstedt, I., Mir, S., Newman, L. E., Oldfield, T. J., Penkett, C. J., Pineda-Castillo, J., Rinaldi, L., Sahni, G., Sawka, G., Sen, S., Slowley, R., da Silva, A. W. S., Suarez-Uruena, A., Swaminathan, G. J., Symmons, M. F., Vranken, W. F., Wainwright, M., and Kleywegt, G. J. (2011) PDBe: Protein Data Bank in Europe. *Nucleic Acids Res. 39*, 402−410.
(26) Pasanen, S., Jänis, J., and Vainiotalo, P. (2007) Cello-, malto- and xylooligosaccharide fragmentation by collision-induced dissociation using QIT and FT-ICR mass spectrometry: a systematic study. *Int. J. Mass Spectrom. 263*, 22−29.
(27) Matthews, B. W. (1968) Solvent content of protein crystals. *J. Mol. Biol. 33*, 491−497.
(28) Krissinel, E., and Henrick, K. (2007) Inference of macromolecular assemblies from crystalline state. *J. Mol. Biol. 372*, 774−797.
(29) Choi, K. H., Lai, V., Foster, C. E., Morris, A. J., Tolan, D. R., and Allen, K. N. (2006) New superfamily members identified for Schiff-base enzymes based on verification of catalytically essential residues. *Biochemistry 45*, 8546−8555.
(30) Daniels, A. D., Campeotto, I., van der Kamp, M. W., Bolt, A. H., Trinh, C. H., Phillips, S. E. V., Pearson, A. R., Nelson, A., Mulholland, A. J., and Berry, A. (2014) Reaction mechanism of N-acetylneuraminic acid lyase revealed by a combination of crystallography, QM/MM simulation, and mutagenesis. *ACS Chem. Biol. 9*, 1025−1032.
(31) Theodossis, A., Walden, H., Westwick, E. J., Connaris, H., Lamble, H. J., Hough, D. W., Danson, M. J., and Taylor, G. L. (2004) The structural basis for substrate promiscuity in 2-keto-3-deoxygluconate aldolase from the Entner-Doudoroff pathway in Sulfolobus solfataricus. *J. Biol. Chem. 279*, 43886−43892.